

References

- 1 Malinowski SM, Pesin SR: Visual field loss caused by retinal vascular occlusion after vitrectomy surgery. *Am J Ophthalmol* 1997;123:707-708.
- 2 Verma L, Venkatesh P, Tewari HK: Combined central retinal artery and central retinal vein occlusion following pars plana vitrectomy. *Ophthalmic Surg Lasers* 1999;30:317-319.
- 3 Melberg NS, Thomas MA: Visual field loss after pars plana vitrectomy with air/fluid exchange. *Am J Ophthalmol* 1995;120:386-388.
- 4 Yan H, Dhurjon L, Chow DR, Williams D, Chen JC: Visual field defect after pars plana vitrectomy. *Ophthalmology* 1998;105:1612-1616.
- 5 Welch JC: Dehydration injury as a possible cause of visual field defect after pars plana vitrectomy for macular hole. *Am J Ophthalmol* 1997;124:698-699.
- 6 Sullivan KL, Brown GC, Forman AR, Sergott RC, Flanagan JC: Retrobulbar anesthesia and retinal vascular obstruction. *Ophthalmology* 1983;90:373-377.
- 7 Cowley M, Campochiaro PA, Newman SA, Fogle JA: Retinal vascular occlusion without retrobulbar or optic nerve sheath hemorrhage after retrobulbar injection of lidocaine. *Ophthalmic Surg* 1988;19:859-861.
- 8 Devoto MH, Kersten RC, Zalta AH, Kulwin DR: Optic nerve injury after retrobulbar anesthesia. *Arch Ophthalmol* 1997;115:687-688.
- 9 Hamilton RC: A discourse on the complications of retrobulbar and peribulbar blockade. *Can J Ophthalmol* 2000;35:363-372.
- 10 Uemura A, Kanda S, Sakamoto Y, Kita H: Visual field defects after uneventful vitrectomy for epiretinal membrane with indocyanine green-assisted internal limiting membrane peeling. *Am J Ophthalmol* 2003;136:252-257.
- 11 Adachi M, Takahashi K, Nishikawa M, Miki H, Uyama M: High intraocular pressure-induced ischemia and reperfusion injury in the optic nerve and retina in rats. *Graefes Arch Clin Exp Ophthalmol* 1996;234:445-451.
- 12 Shinoda K, Ohde H, Ishida S, Kawashima S, Kitamura S, Mita S, Inoue M, Katsura H: A case of proliferative diabetic retinopathy with development of ischemic optic neuropathy after pars plana vitrectomy [in Japanese]. *Folia Ophthalmol Jpn* 2000;51:925-929.
- 13 Miyake Y, Hirose T, Hara A: Electrophysiologic testing of visual functions for vitrectomy candidates. I. Results in eyes with known fundus diseases. *Retina* 1983;3:86-94.
- 14 Hood DC, Bach M, Brigell M, Keating D, Kondo M, Lyons JS, Palmowski-Wolfe AM: ISCEV guidelines for clinical multifocal electroretinography (2007 edition). *Doc Ophthalmol* 2008;116:1-11.
- 15 Betsuin Y, Mashima Y, Ohde H, Inoue R, Oguchi Y: Clinical application of the multifocal VEPs. *Curr Eye Res* 2001;22:54-63.
- 16 Khwarg SG, Linstone FA, Daniels SA, Isenberg SJ, Hanscom TA, Geoghegan M, Straatsma BR: Incidence, risk factors, and morphology in operating microscope light retinopathy. *Am J Ophthalmol* 1987;103:255-263.
- 17 McDonald HR, Harris MJ: Operating microscope-induced retinal phototoxicity during pars plana vitrectomy. *Arch Ophthalmol* 1988;106:521-523.
- 18 Pendergast SD, McCuen BW 2nd: Visual field loss after macular hole surgery. *Ophthalmology* 1996;103:1069-1077.
- 19 Hayreh SS: Anterior ischemic optic neuropathy. IV. Occurrence after cataract extraction. *Arch Ophthalmol* 1980;98:1410-1416.
- 20 Jayam AV, Hass WK, Carr RE, Kumar AJ: Saturday night retinopathy. *J Neurol Sci* 1974;22:413-418.
- 21 Boldt HC, Munden PM, Folk JC, Mehaffey MG: Visual field defects after macular hole surgery. *Am J Ophthalmol* 1996;122:371-381.
- 22 Becker H, Schmitz J: Computer-assisted quantitative-static perimetry following panretinal argon laser coagulation in diabetic retinopathy [in German]. *Klin Monbl Augenheilkd* 1998;192:204-207.
- 23 Hidayat AA, Fine BS: Diabetic choroidopathy. Light and electron microscopic observations of seven cases. *Ophthalmology* 1985;92:512-522.
- 24 Kroll P, Wiegand W, Schmidt J: Vitreopapillary traction in proliferative diabetic vitreoretinopathy. *Br J Ophthalmol* 1909;83:261-264.
- 25 Langham ME, Grebe R, Hopkins S, Marcus S, Sebag M: Choroidal blood flow in diabetic retinopathy. *Exp Eye Res* 1991;52:167-173.

- 26 Taban M, Lewis H, Lee MS: Nonarteritic anterior ischemic optic neuropathy and 'visual field defects' following vitrectomy: could they be related? *Graefes Arch Clin Exp Ophthalmol* 2007;245:600-605.
- 27 Klistorner AI, Graham SL, Grigg JR, Billson FA: Multifocal topographic visual evoked potential: improving objective detection of local visual field defects. *Invest Ophthalmol Vis Sci* 1998;39:937-950.
- 28 Viswanathan S, Frishman LJ, Robson JG, Harwerth RS, Smith EL 3rd: The photopic negative response of the macaque electroretinogram: reduction by experimental glaucoma. *Invest Ophthalmol Vis Sci* 1999;40:1124-1136.
- 29 Gotoh Y, Machida S, Tazawa Y: Selective loss of the photopic negative response in patients with optic nerve atrophy. *Arch Ophthalmol* 2004;122:341-346.
- 30 Frishman LJ: Origins of the electroretinogram; in Heckenlively JR, Arden GB (eds): *Principle and Practice of Clinical Electrophysiology of Vision*, ed 2. Cambridge, Mass., The MIT Press, 2006, pp 139-183.

This is an Open Access article licensed under the terms of the Creative Commons Attribution-NonCommercial-NoDerivs 3.0 License (www.karger.com/OA-license), applicable to the online version of the article only. Distribution for non-commercial purposes only.

Tissue Plasminogen Activator-Assisted Vitrectomy for Ruptured Eye with Suprachoroidal Hemorrhage

Koichi Matsumoto Celso Soiti Matsumoto Kei Shinoda
Emiko Watanabe Atsushi Mizota

Department of Ophthalmology, Teikyo University School of Medicine,
University Hospital Itabashi, Tokyo, Japan

Key Words

Tissue plasminogen activator · Suprachoroidal hemorrhage · Rupture · Ocular injury

Abstract

Purpose: To report a case of a ruptured eye with a suprachoroidal hemorrhage (SCH) in which tissue plasminogen activator (tPA)-assisted vitrectomy was successful in reconstructing the globe and restoring good vision.

Case: A 32-year-old man was struck on the right eye by a surfboard. His eye was ruptured and his visual acuity decreased to hand movements. Surgery was immediately performed to successfully close the ruptured globe. Nine days later, a second surgery was performed, and tPA (25 µg/0.1 ml monteplase) was used to liquefy and drain the SCH. This freed enough vitreous space for a more comprehensive vitrectomy. Eighteen months after the injury, the retina remained attached, and the decimal best-corrected visual acuity improved to 0.8.

Conclusion: tPA was helpful in lysing a massive SCH, thereby contributing to the excellent visual outcome. tPA-assisted drainage should be considered in cases of massive SCH when drainage is difficult due to an incomplete lysis of the clot.

Introduction

A suprachoroidal hemorrhage (SCH) in eyes with a ruptured globe is one of the causes of poor visual prognosis especially when it is massive and involves the macula [1, 2]. The SCH is generally drained one to two weeks after the injury when the clot has lysed. A freely moving blood clot in the suprachoroidal space in the dynamic B-mode ultrasonographic images indicates that SCH drainage can be accomplished during intraocular surgery [2]. However, the entire clot does not dissipate simultaneously, and

residual solid clots result in incomplete drainage and may hamper further procedures, such as pars plana vitrectomy, for repairing a retinal detachment (RD).

Recently, successful drainage of a subretinal hemorrhage in eyes with age-related maculopathy (AMD) during vitrectomy with the injection of tissue plasminogen activator (tPA) has been obtained [3]. We present a patient with a ruptured globe with a massive SCH where a tPA-assisted vitrectomy was successful in removing the SCH, which allowed the reconstruction of the posterior pole of the eye to attain good visual outcome.

Case Report

A 32-year-old man was struck on the right eye by a surfboard which ruptured the globe, and his visual acuity was reduced to hand movement vision. Surgery was immediately performed to close the open globe. Intraoperatively, a Y-shaped laceration was found between the lateral and inferior rectus muscles approximately 15 mm posterior to the limbus (fig. 1). The lateral rectus muscle was temporally disinserted, and the wound was closed with several interrupted 8-0 nylon sutures. The muscle was sutured back to the site of the original insertion.

Postoperatively, a dense hyphema hampered the view of the fundus. Computed tomography showed a massive suprachoroidal hemorrhage that occupied about 3/4 of the vitreous cavity in the nasal and superior space (fig. 1).

Nine days after the injury, a second surgery was performed with a choroidal tap, lensectomy, pars plana vitrectomy, and an encircling scleral band. After lens aspiration, a 25-gauge irrigation cannula was placed in the anterior chamber to control the intraocular pressure, and a posterior sclerotomy for drainage was created 12 mm posterior to the limbus in the superior nasal quadrant. Because the firm SCH clot did not permit easy drainage, tPA (25 µg/0.1 ml monteplase) was injected into the suprachoroidal space (online suppl. video 1; see www.karger.com/doi/10.1159/000342136 for all online suppl. videos) from sclerotomy site using a 27-gauge blunt needle. Sixty minutes later, several smaller clots were extracted from the sclerotomy drainage site (online suppl. video 2), and the vitreous cavity was larger and relatively clear. This permitted standard 3-port vitrectomy to be performed. First, the vitreous hemorrhage was removed, and the clear view of the retina allowed us to detect a RD. The retina was reattached by drainage of the subretinal fluid, and an encircling with silicone band. Then a small amount of silicone oil was injected because part of the vitreous cavity was still occupied by the reduced SCH (fig. 2). The residual SCH was gradually absorbed and was not detected 34 days after the injury.

On day 70 after the injury, the silicone oil was removed but two days later the retina re-detached. Additional vitrectomy with SF₆ tamponade and intraocular lens suturing were performed on day 77 after the injury. Sixteen months after the injury, the retina was still attached and the visual acuity had improved to 0.8 with a correction of -3.50 diopter lens (fig. 2).

Discussion

Our results showed that a two-step surgical strategy can lead to good visual outcomes for open-globe injuries accompanied by a large SCH involving the macula. The initial surgery is performed immediately to close the open eye, and after about two weeks when the SCH is moveable, the second surgery is performed to treat the posterior pathology [1, 2]. The time of the combined SCH drainage through the sclerotomy and pars plana vitrectomy for secondary RD is critical. Incomplete lysis of the clot may lead to difficulty in clearing the vitreous cavity to perform surgery on the

retina, e.g., repairing a RD. Failure to obtain a clear view of the retina can also lead to relative poor visual outcomes especially when the SCH is massive [1, 2].

At present, tPA-assisted drainage or displacement of subretinal hemorrhages in eyes with AMD or retinal macroaneurysms is commonly performed. Animal experiments have shown the efficacy of tPA in treating experimental SCHs [4], but thus far, only a single case has been reported where tPA was used to assist in the drainage of a SCH [5]. The results of our case showed that injection of tPA into the SCH led to a lysis of the clot that led to a smooth drainage of the SCH. Thus, we recommend that tPA be used in eyes with a large SCH when drainage is difficult due to incomplete lysis of the clot.

Acknowledgements

Support of this study was provided by Researches on Sensory and Communicative Disorders from the Ministry of Health, Labor, and Welfare, Japan. No author has a proprietary interest in any material or method mentioned.

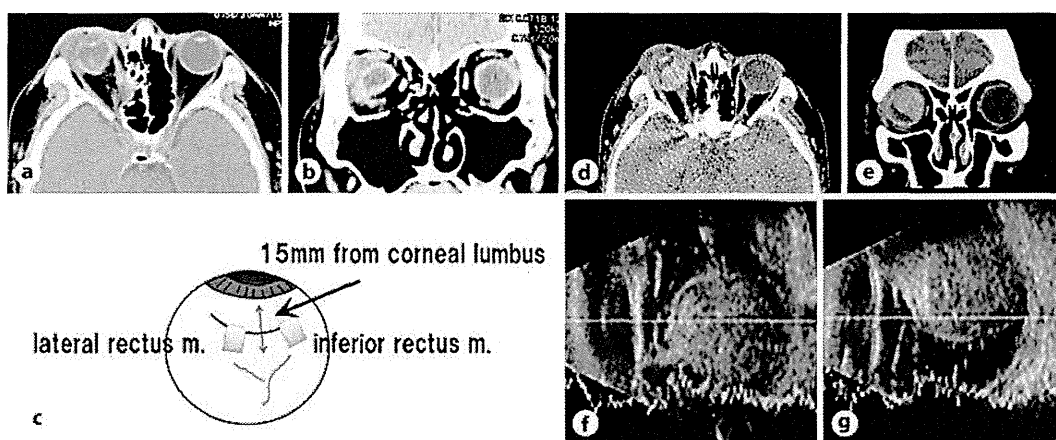


Fig. 1. Computed tomography (CT), B mode ultrasonography (B-mode echo), and a scheme showing intraoperative findings of the primary surgery for an open-globe injury. **a, b** Coronal (**a**) and transverse (**b**) images showing distorted right eye globe and orbital fracture. **c** A Y-shaped wound can be seen between the lateral and inferior rectus muscles and approximately 15 mm behind the limbus. The lateral rectus muscle was temporarily removed and sutured back to the original insertion site after the wound was closed with several interrupted sutures by 8-0 nylon. **d, e** Coronal (**d**) and transverse (**e**) CT images taken on day 4 after the primary surgery. **f, g** Horizontal (**f**) and vertical (**g**) sectioned B-mode echo images taken 3 days after the primary surgery. Massive suprachoroidal hemorrhage occupied about 3/4 of the vitreous cavity at the nasal and superior space.

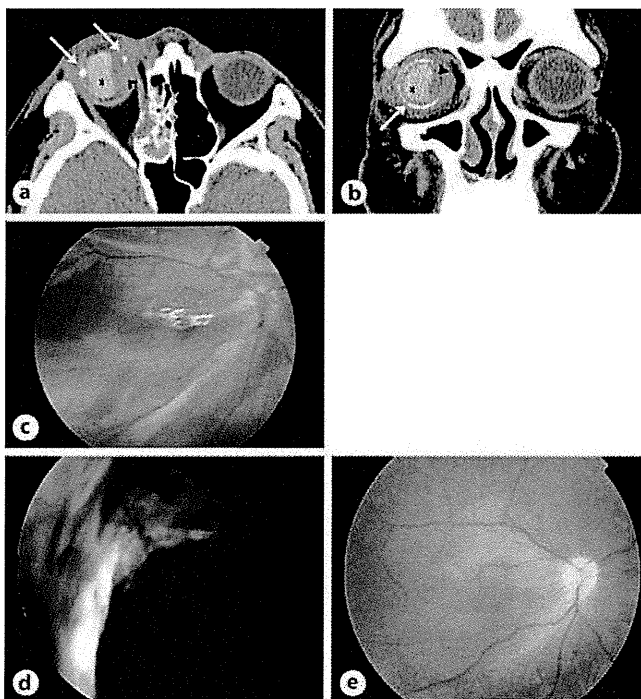


Fig. 2. Computed tomography (CT) and fundus photograph after the second surgery. **a, b** Transversely (**a**) and coronally (**b**) sectioned CT images taken 3 days after the second surgery showing that a clot (arrowhead) has been reduced. Arrows indicate encircling band and asterisk indicates silicone oil (S.O.). **c** Fundus photograph of the right eye taken 15 days after the second surgery showing attached retina under S.O. tamponade and subretinal hemorrhage. Best-corrected visual acuity (BCVA) was 0.07. **d, e** Fundus photograph of the right eye taken 7 months after the second surgery showing attached retina without any vitreous substitute. BCVA was 0.8.

References

- 1 Meier P, Wiedemann P: Massive suprachoroidal hemorrhage: secondary treatment and outcome. *Graefes Arch Clin Exp Ophthalmol* 2000;238:28–32.
- 2 Chu TG, Cano MR, Green RL, Liggett PE, Lean JS: Massive suprachoroidal hemorrhage with central retinal apposition. A clinical and echographic study. *Arch Ophthalmol* 1991;109:1575–1581.
- 3 Kamei M, Estafanous M, Lewis H: Tissue plasminogen activator in the treatment of vitreoretinal diseases. *Semin Ophthalmol* 2000;15:44–50.
- 4 Kwon OW, Kang SJ, Lee JB, Lee SC, Yoon YD, Oh JH: Treatment of suprachoroidal hemorrhage with tissue plasminogen activator. *Ophthalmologica* 1998;212:120–125.
- 5 Murata T, Kikushima W, Imai A, Toriyama Y, Tokimitsu M, Kurokawa T: Tissue-type plasminogen activator-assisted drainage of suprachoroidal hemorrhage showing a kissing configuration. *Jpn J Ophthalmol* 2011;55:431–432.

This is an Open Access article licensed under the terms of the Creative Commons Attribution-NonCommercial-NoDerivs 3.0 License (www.karger.com/OA-license), applicable to the online version of the article only. Distribution for non-commercial purposes only.

Case of Unilateral Peripheral Cone Dysfunction

Yujin Mochizuki^a Kei Shinoda^b Celso Soiti Matsumoto^b
Gerd Klose^c Emiko Watanabe^b Keisuke Seki^b
Itaru Kimura^a Atsushi Mizota^b

^aDepartment of Ophthalmology, Juntendo University Urayasu Hospital, Chiba,

^bDepartment of Ophthalmology, Teikyo University School of Medicine, University Hospital Itabashi, and ^cCarl Zeiss Meditec Co., Ltd., Tokyo, Japan

Key Words

Tunnel vision · Electroretinogram · Multifocal ERG · Optical coherence tomography · Pattern visual evoked potentials

Abstract

Purpose: Peripheral cone dystrophy is a subgroup of cone dystrophy, and only 4 cases have been reported. We present a patient with unilateral peripheral cone dysfunction and report the functional changes determined by electrophysiological tests and ultrastructural changes determined by spectral domain optical coherence tomography (SD-OCT).

Case: A 34-year-old woman complained of blurred vision in both eyes. Our examination showed that her visual acuity was 0.05 OD and 0.2 OS. A relative afferent pupillary defect was present in her right eye. The results of slit-lamp examination, ophthalmoscopy, and fluorescein angiography were normal except for pallor of the right optic disc. SD-OCT showed a diffuse thinning of the retina in the posterior pole of the right eye. A severe constriction of the visual fields was found in both eyes but more in the right eye. The photopic full-field electroretinograms (ERGs) were reduced in the right eye but normal in the left eye. The multifocal ERGs were severely reduced throughout the visual field except in the central area of the right eye. The multifocal ERGs from the left eye were normal. The pattern visual evoked responses were within the normal range in both eyes. She had a 5-year history of sniffing paint thinner.

Results: Although the visual dysfunction was initially suspected to be due to psychological problems from the results of subjective tests, objective tests indicated a peripheral cone dysfunction in the right eye. The pathophysiological mechanism and the relationship with thinner sniffing were not determined.

Conclusions: Our findings indicate that peripheral cone dysfunction can occur unilaterally. Electrophysiology and SD-OCT are valuable tests to perform to determine the pathogenesis of unusual ocular findings objectively.

Introduction

An inherited central cone dysfunction was named occult macular dystrophy (OMD) or Miyake's disease [1–3], and the gene responsible for OMD has been identified [4]. In OMD, only the central cone function is abnormal. There are also cases where only the peripheral cone functions are abnormal while the central cone function is normal. However, these cases are rare and only four cases of peripheral cone dysfunction have been reported. In these cases, the rod function is normal over the entire retina [5, 6]. Kondo et al. [5] first described peripheral cone dystrophy, and they carefully analyzed focal areas of the central retina in 3 patients with peripheral cone dystrophy. They showed that the dysfunction of the cones was predominantly in the periphery and the central area was relatively well preserved. Okuno et al. [6] reported an elderly man with bilateral peripheral cone dystrophy, and the patient's signs and symptoms had not changed for over 50 years. Therefore they concluded that such condition in their case was not a manifestation of an early stage of the more common type of cone dystrophy.

We present a patient with peripheral cone dysfunction but the abnormalities were found in only one eye. In addition to the unilateral dystrophy, the patient had several features that were different from previous cases of peripheral cone dystrophy.

Case Report

A 34-year-old Japanese woman complained of a gradually decrease of her vision in both eyes. She visited a neighborhood eye clinic on December 2008, and the examination showed that her best-corrected decimal visual acuity (BCVA) was 0.3 OD and 0.5 OS. A diagnosis was not made, and she was not treated. Three months later she was referred to our clinic. She reported that she had noticed that her right visual field had been constricted for 10 years. She did not complain of photopsia, photophobia, night blindness, or color vision disturbances. She had a history of paint thinner sniffing of more than 5 years. Our examination showed that her BCVA was 0.05 OD and 0.2 OS. The results of slit-lamp biomicroscopy, ophthalmoscopy, and fluorescein angiography were normal except for right optic disc pallor (fig. 1). Goldman and Humphrey visual field tests showed a concentric constriction of the visual fields in both eyes but more severe in the right eye (fig. 1). A relative afferent pupillary defect was present in the right eye. Brain magnetic resonance imaging showed no abnormalities.

The amplitudes of the full-field scotopic b-waves of the ERGs were reduced in both eyes (fig. 2), and that of the mixed rod:cone ERGs were also reduced. The oscillatory potentials (OPs) and the photopic cone ERGs were unrecordable in the right eye, i.e., less than the noise level (5 μ V for OPs and 20 μ V for the photopic cone ERGs), and the flicker ERGs were highly attenuated by approximately 95% of that of the right eye. The responses from the left eye were essentially normal except that the amplitude of the scotopic rod ERGs was at the lower limit of the normal range.

The multifocal ERGs (mfERGs; fig. 2, online suppl. table 1; for all online suppl. material, see www.karger.com/doi/10.1159/000339129) were well preserved in the central retina but severely reduced in the periphery of the right eye. These findings were in good accordance with the results of perimetry. The mfERGs were well preserved in all areas of the left eye. The mfERGs from each concentric ring were summed and analyzed. This showed that only the central responses were preserved in the right eye, and no significant difference of the implicit time was found in the central area between the two eyes. Pattern visual evoked response was within normal limits in both eyes (fig. 2).

Microstructural images of the fovea were obtained by the SD-OCT (OCT4000, Cirrus HD-OCT, Carl Zeiss Medinc Inc., Dublin, Calif., USA). The 3D datasets were obtained using the raster scan protocol of 128 horizontal B-scan images, each composed of 512 axial scans. This raster scan protocol covered an area of 6 mm (horizontal) \times 6 mm (vertical) \times 1.7 mm (axial) with a horizontal pixel spacing of 11 μ m (6 mm/512) and a vertical pixel spacing of 47 μ m (6 mm/128).

High-quality images of 9 mm horizontal and 6 mm vertical scans were obtained using the HD 5-line raster scan protocol of 5 B-scan images, each composed of 1,024 axial scans. Each B-scan was acquired with 4-times oversampling and subsequent pixel profiling to obtain noise-reduced images. This raster scan protocol examines the cross section of B-scans through the fovea with a horizontal pixel spacing of 9 μm (9 mm/1,024) and a vertical pixel spacing of 6 μm (6 mm/1,024).

Based on the HD 5-line raster scans in the horizontal and vertical orientation of both the right and left eye, the outer nuclear layer (ONL) could be identified and its thickness determined. The thickness of the ONL was defined as the vertical distance between the highly reflective line corresponding to the external limiting membrane (ELM) and the midpoint of the transition from the highly reflective outer plexiform layer (OPL) to the less reflective ONL. Manual thickness measurements were made at many points on the central horizontal and vertical B-scan cross sections (online suppl. fig. 1) using the built-in caliper tool. In addition, the images were analyzed with the help of an external mathematical program to automatically detect the ONL boundaries and determine the layer thickness. The thickness values have been averaged over segments of 1 mm length, corresponding to the popular EDTRS grid.

In general, the configuration and microstructure in the macula were normal in both eyes; the ELM, the photoreceptor inner and outer segment (IS/OS) lines, and the foveal bulge were distinct in the SD-OCT images in both eyes (fig. 1). However, comparisons of each layer between the two eyes showed a diffuse thinning of the retina especially the ONL in the extramacular area of the right eye. Online supplementary table 2 summarizes the quantitative results obtained from the manual and automated thickness analysis.

Discussion

Peripheral cone dystrophy is a very rare clinical entity, and its clinical characteristics have been presented in only two publications [5, 6]. The possibility of having patients with peripheral cone dystrophy or patients with similar characteristics has been discussed [7–10]. However, these authors did not compare the central and peripheral cone function and also did not demonstrate that the rod system was functioning normally across the retina.

Recent developments of the clinical techniques of evaluating retinal function in localized areas, e.g., focal ERGs, mfERGs, and rod and cone perimetry, have allowed assessments of central [1–3] or peripheral cone dysfunction [5, 6]. The etiology of the findings of our case is unknown. Inherited diseases, vascular disease, systemic disease, infection, inflammation, and an exposure to toxins were considered in the differential diagnosis. Our case had a history of paint thinner sniffing, and thus the results of subjective testing should be carefully interpreted. However, the electrophysiological findings including full-field ERGs, mfERGs, and visual evoked potentials clearly showed diffuse cone dysfunction except in the central area of only the right eye. On the other hand, rod in the right eye, both rod and cone in the left eye, and optic nerve functioned well in both eyes. Moreover microstructural analysis on the retina supports these objective functional results. However, the severely decreased visual acuity and highly constricted visual field in both eyes do not agree with our diagnosis of peripheral cone dystrophy. These contradictory findings might be because our patient had psychogenic disorders induced by thinner sniffing and the possibility of unilaterally pronounced toxic effects cannot be denied [11]. But thinner sniffing has been reported to lead to mainly optic neuropathy [12, 13] but the normal visual evoked potentials of our patient indicated that this was not likely.

Another differential diagnosis of our case is acute zonal occult outer retinopathy (AZOOR) which is a uni- or bilateral disease characterized by an acute zonal loss of

outer retinal function with minimal ophthalmoscopic changes [14]. Recently, local retinal microstructure assessed by Fourier-domain and spectral-domain optical coherence tomography showed that the major OCT findings in this disease were the selective absence or discontinuity of the IS/OS line and the cone outer segment tip (COST) line in the retinal areas corresponding to the functional decrease [15, 16]. Defect of the IS/OS line and thinning of the ONL has been reported in AZOOR [17, 18]. In our case, the onset was not acute according to the patient's description, but otherwise the clinical manifestations are compatible to AZOOR clinical entity. However, we believe that our case was not AZOOR because the IS/OS line appeared normal in the area with severely reduced mfERGs in the right eye, and a unilateral, diffuse, peripheral, cone-selective dysfunction in AZOOR has not been reported.

Microstructural analyses showed a selective thinning of the ONL with the outer plexiform layer and IS/OS line intact. These findings are in good agreement with the severe attenuation of the a-wave in photopic ERG and mfERG. This supports the idea of a selective cone dysfunction.

Only five cases of unilateral cone dysfunction have been reported [19–22]. Two cases from Sieving [19] had normal rod ERGs in both eyes but reduced cone ERGs in only one eye. He reported abnormally prolonged b-wave when long-duration photopic flashes were used, and these abnormalities were ascribed to the hyperpolarizing bipolar and/or horizontal cells. In contrast, our subject had no measurable full-field photopic ERGs. The other three cases, a 19-year-old woman reported by Zervas and Smith [20], a 53-year-old woman by Brigell and Celesia [21], and a 20-year-old woman by Nomura et al. [22], had unilateral severe cone dysfunction while the rod function was intact in both eyes, which is similar with our case. But all three cases had an acute onset and the 20-year-old woman demonstrated bull's eye maculopathy three months later. The two cases from Zervas and Smith, and Brigell and Celesia had good visual acuity and ophthalmoscopically normal macula in the affected eye. Although information about focal macular ERGs was not reported in these cases, the abnormal full-field ERGs and preserved macular function appear similar to our case, except that our case had severely reduced visual acuity.

Considering all of our findings, we conclude that our case had unilateral peripheral cone dysfunction, and the findings are different from those of the more common cone dystrophy as well as of the reported cases with peripheral cone dystrophy.

Disclosure Statement

No author has a financial or proprietary interest in any material or method mentioned except that G.K. is employed at Carl Zeiss Meditec Co., Ltd., Japan (support limited to not-commercially available data analysis). Support of this study was provided by Research Grants on Sensory and Communicative Disorders from the Ministry of Health, Labor, and Welfare, Japan.

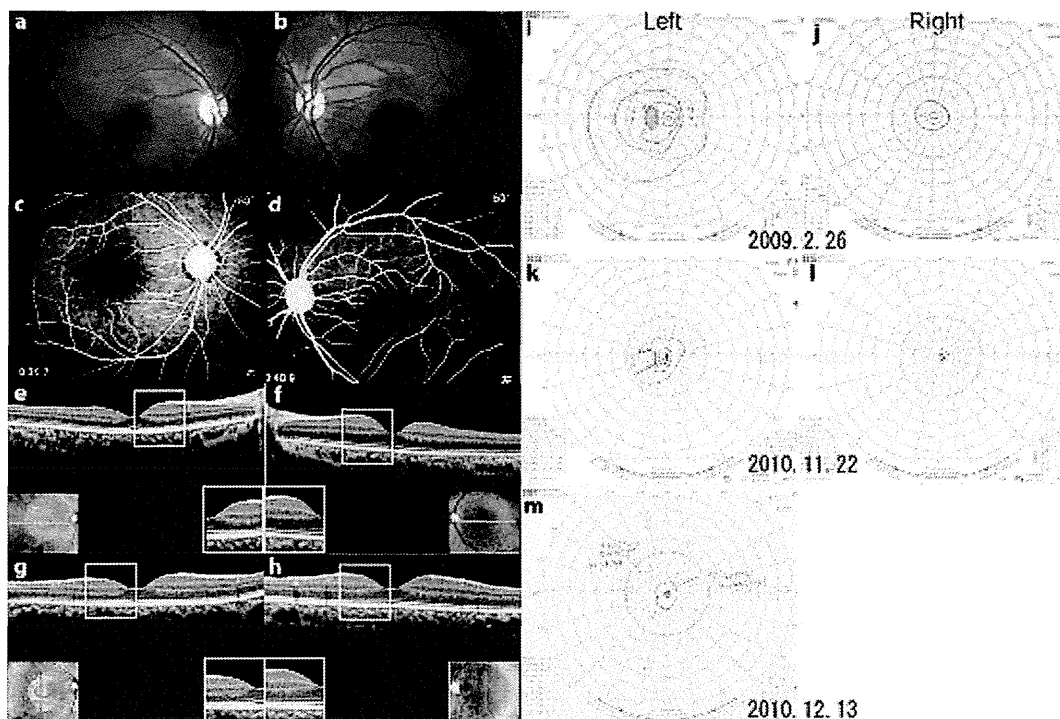


Fig. 1. Fundus photographs, fluorescein angiograms, visual fields, and optical coherence tomographic (OCT) images from our patient with unilateral peripheral cone dystrophy. **a–d** Fundus photographs and fluorescein angiograms showing no abnormal findings. **e–h** OCT images from a 9-mm horizontal scan of the right (**e**) and left (**f**) eyes and vertical scan in the right (**g**) and left (**h**) eyes. Note that the outer nuclear layer is thinner in the right eye than that in the left eye in large areas of the retina except the fovea (*inset*). **i–m** Goldmann visual fields showing bilateral constriction of the visual fields in both eyes but more severe in the right eye.

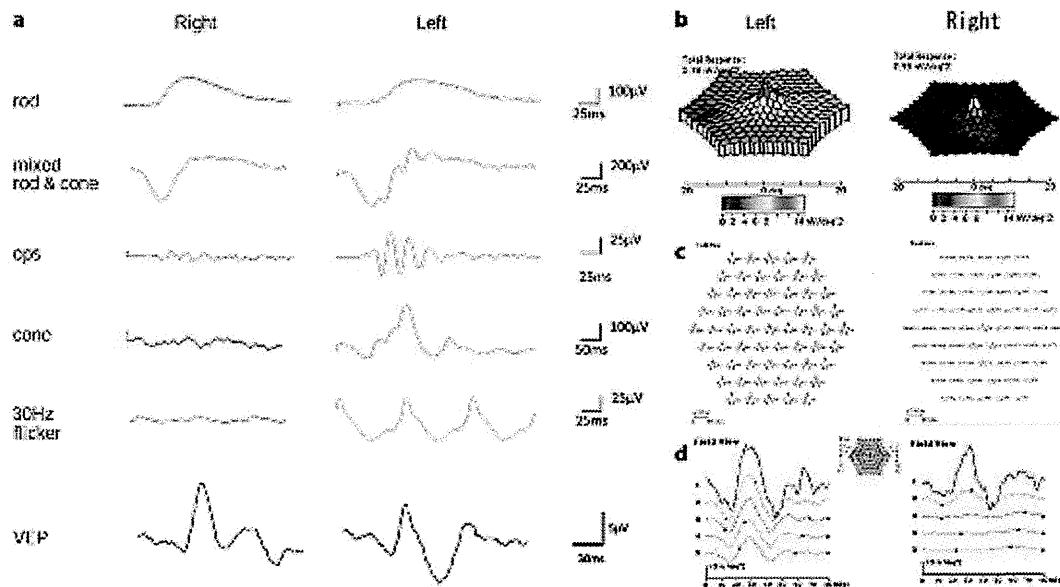


Fig. 2. Full-field and multifocal electroretinograms (ERGs) recorded from our patient with unilateral peripheral cone dystrophy. Full-field ERG showed that rod responses are symmetrical in both eyes, but the responses of cone system are flat in the right eye while normal in the left eye. The multifocal ERGs are severely attenuated in the peripheral retinal area while that from the central area is normal in the right eye. The response density in the left eye was normal.

References

- Miyake Y, Ichikawa K, Shiose Y, Kawase Y: Hereditary macular dystrophy without visible fundus abnormality. *Am J Ophthalmol* 1989;108:292–299.
- Miyake Y, Horiguchi M, Tomita N, Kondo M, Tanikawa A, Takahashi H, Suzuki S, Terasaki H: Occult macular dystrophy. *Am J Ophthalmol* 1996;122:644–653.
- Miyake Y: *Electrodiagnosis of Retinal Disease*. Tokyo, Springer-Verlag, 2006.
- Akahori M, Tsunoda K, Miyake Y, Fukuda Y, Ishiura H, Tsuji S, Usui T, Hatase T, Nakamura M, Ohde H, Itabashi T, Okamoto H, Takada Y, Iwata T: Dominant mutations in RP1L1 are responsible for occult macular dystrophy. *Am J Hum Genet* 2010;87:424–429.
- Kondo M, Miyake Y, Kondo N, Ueno S, Takakuwa H, Terasaki H: Peripheral cone dystrophy: a variant of cone dystrophy with predominant dysfunction in the peripheral cone system. *Ophthalmology* 2004;111:732–739.
- Okuno T, Oku H, Kurimoto T, Oono S, Ikeda T: Peripheral cone dystrophy in an elderly man. *Clin Experiment Ophthalmol* 2008;36:897–899.
- Krill AE, Deutman AF, Fishman M: The cone degenerations. *Doc Ophthalmol* 1973;35:1–80.
- Pinckers A, Deutman AF: Peripheral cone disease. *Ophthalmologica* 1977;174:145–150.
- Pearlman JT, Owen WG, Brounley DW, Sheppard JJ: Cone dystrophy with dominant inheritance. *Am J Ophthalmol* 1974;77:293–303.
- Noble KG, Siegel IM, Carr RE: Progressive peripheral cone dysfunction. *Am J Ophthalmol* 1988;106:557–560.
- Toyonaga N, Adachi-Usami E, Yamazaki H: Clinical and electrophysiological findings in three patients with toluene dependency. *Doc Ophthalmol* 1989;73:201–207.
- Kohriyama K, Hori H, Murai Y, Ninomiya H, Tsukamoto Y: Optic neuropathy induced by thinner sniffing. *J UOEH* 1989;11:449–453.

- 13 Poblano A, Lope Huerta M, Martínez JM, Falcón HD: Pattern-visual evoked potentials in thinner abusers. *Arch Med Res* 1996;27:531-533.
- 14 Gass JD: Acute zonal occult outer retinopathy. Donders Lecture: The Netherlands Ophthalmological Society, Maastricht, Holland, June 19, 1992. *J Clin Neuroophthalmol* 1993;13:79-97.
- 15 Park SJ, Woo SJ, Park KH, Hwang JM, Chung H: Morphologic photoreceptor abnormality in occult macular dystrophy on spectral-domain optical coherence tomography. *Invest Ophthalmol Vis Sci* 2010;51:3673-3679.
- 16 Sugahara M, Shinoda K, Matsumoto CS, Satofuka S, Hanazono G, Imamura Y, Mizota A: Outer retinal microstructure in a case of acute idiopathic blind spot enlargement syndrome. *Case Report Ophthalmol* 2011;2:116-122.
- 17 Spaide RF, Koizumi H, Freund KB: Photoreceptor outer segment abnormalities as a cause of blind spot enlargement in acute zonal occult outer retinopathy-complex diseases. *Am J Ophthalmol* 2008;146:111-120.
- 18 Ohta K, Sato A, Fukui E: Spectral domain optical coherence tomographic findings at convalescent stage of acute zonal occult outer retinopathy. *Clin Ophthalmol* 2009;3:423-428.
- 19 Sieving PA: Unilateral cone dystrophy: ERG changes implicate abnormal signaling by hyperpolarizing bipolar and/or horizontal cells. *Trans Am Ophthalmol Soc* 1994;92:459-471; discussion 471-474.
- 20 Zervas JP, Smith JL: Neuro-ophthalmic presentation of cone dysfunction syndromes in the adult. *J Clin Neuroophthalmol* 1987;7:202-218.
- 21 Brigell M, Celesia GG: Electrophysiological evaluation of the neuro-ophthalmology patient: an algorithm for clinical use [review]. *Semin Ophthalmol* 1992;7:65-78.
- 22 Nomura R, Kondo M, Tanikawa A, Yamamoto N, Terasaki H, Miyake Y: Unilateral cone dysfunction with bull's eye maculopathy. *Ophthalmology* 2001;108:49-53.



Novel Mutations in Enhanced S-cone Syndrome

Dear Editor:

Enhanced S-cone syndrome (ESCS) is a rare and unique retinal dystrophy with a pattern of autosomal-recessive inheritance.¹⁻³ Patients with ESCS show night blindness and high sensitivity to short-wavelength light, because of the 2-fold increased number of short-wavelength-sensitive cones (S cones) with absence of rods in the retina. Since the first discovery of mutations in the *NR2E3* gene on chromosome 15q23 in patients with ESCS,⁴ >40 mutations have been reported as causes of ESCS and allied diseases (Fig 1, available online at <http://aaojournal.org>).

In this letter, we report novel mutations in the *NR2E3* gene that were discovered in 2 cases with ESCS.

Cases are 2 Japanese patients who were reported previously.³ Case 1 was a 31-year-old man whose parents were consanguineous. His vision was 0.7 in the right eye and 0.3 in the left eye. Funduscopy revealed retinal degeneration surrounding the vascular arcade with cystic changes in both maculae (Fig 2, available online at <http://aaojournal.org>). Perimetry showed ring-shaped scotoma and electrophysiology showed unique responses corresponding to ESCS (Figs 3–6, available online at <http://aaojournal.org>). During 23-year clinical follow-up, clumped pigmentation has appeared in the retinal degeneration and the cystic changes in the foveal region have become ambiguous (Fig 2). His latest vision was 0.5 in the right eye and 0.3 in the left eye at age 53.

Genetic analysis revealed a novel nucleotide substitution (c.151G>A) in exon 2 homozygously, resulting in a novel missense mutation (a glycine-to-arginine substitution) at amino acid position 51 (p.G51R; Fig 7; available online at <http://aaojournal.org>).

Case 2 was a 78-year-old woman.³ Funduscopy showed diffuse mild retinal degeneration with no pigmentation in both eyes (Fig 8, available online at <http://aaojournal.org>). Optical coherence tomography showed a subtle foveal schisis in the left eye, although the structure of the retina including the outer nuclear layer in the macular area was relatively well maintained (Fig 8). After cataract surgery, her vision improved to 0.3 in the right eye and 0.2 in the left.

Genetic analysis revealed compound heterozygous mutations of c.142C>T (exon 2) and c.311G>A (exon 3), resulting in an arginine-to-cysteine substitution at amino acid position 48 (p.R48C) and an arginine-to-glutamine substitution at amino acid position 104 (p.R104Q; Fig 7).

A daughter of case 2 who was asymptomatic and had normal fundus appearance showed only the p.R48C mutation heterozygously, that indicated she was an unaffected carrier relative (Fig 7).

NR2E3 protein, a photoreceptor-specific orphan nuclear receptor, plays an important role in the development and differentiation of rods and all cone classes. NR2E3 has 2 functionally important domains, namely, the DNA-binding domain (DBD) and the ligand-binding domain (Fig 1). Mutations within these domains result in serious dysfunction of NR2E3 protein leading to abnormal process of development and differentiation of multipotent progenitor cells to rods and cones.

Genetic analysis revealed a homozygous mutation (p.G51R) in case 1 and compound heterozygous mutations of (p.R48C) and (p.R104Q) in case 2. Among these mutations, (p.G51R) and (p.R48C) are novel as causative mutations of ESCS.

The mutation (p.G51R) found in case 1 resides in the first zinc finger of the DBD, and the compound heterozygous mutations (p.R48C and p.R104Q), which were found in case 2 reside in the first and second zinc fingers of the DBD. Because the zinc fingers are necessary for maintenance the structure of NR2E3 protein, these mutations in the zinc fingers of NR2E3 result in phenotypes as ESCS (Fig 1).

Clinically, case 1 with a homozygous missense mutation (p.G51R) showed typical features as ESCS, whereas case 2 with compound heterozygous mutations (p.R48C and p.R104Q) showed mild retinal degeneration and has kept some level of vision and construction of the macula despite advanced age. In the past, the mutation (p.R104Q) has never been reported except in 1 case, which demonstrated the normal structure and function of the macula with recordable rod electrophysiology.⁵ These facts indicate the mutation (p.R104Q) may be correlated with the relatively mild clinical findings as ESCS.

We identified 2 novel missense mutations (p.G51R and p.R48C) as causes of ESCS. To our knowledge, the finding of case 1 is the longest-observed clinical case ever reported, and case 2 is the oldest case among all the patients with ESCS so far reported.

KAZUKI KUNIYOSHI, MD,¹ TAKA AKI HAYASHI, MD,² HIROYUKI SAKURAMOTO, MD,¹ AKIRA NAKAO, MD,¹
TAKASHI SATO, MD,¹ TOMOHIRO UTSUMI,² HIROSHI TSUNEOKA, MD,² YOSHIKAZU SHIMOMURA, MD¹

¹Department of Ophthalmology, Kinki University, Faculty of Medicine, Osaka, Japan; ²Department of Ophthalmology, The Jikei University School of Medicine, Tokyo, Japan

References

- Marmor MF, Jacobson SG, Foerster MH, et al. Diagnostic clinical findings of a new syndrome with night blindness, maculopathy, and enhanced S cone sensitivity. *Am J Ophthalmol* 1990;110:124–34.
- Jacobson SG, Marmor MF, Kemp CM, Knighton RW. SWS (blue) cone hypersensitivity in a newly identified retinal degeneration. *Invest Ophthalmol Vis Sci* 1990;31:827–38.
- Sato T, Kuniyoshi K, Nakao A, et al. Long-term observation of two cases of enhanced S-cone syndrome. *J Jpn Ophthalmol Soc* 2009;113:980–90.
- Haider NB, Jacobson SG, Cideciyan AV, et al. Mutation of a nuclear receptor gene, *NR2E3*, causes enhanced S cone syndrome, a disorder of retinal cell fate. *Nat Genet* 2000;24:127–31.
- Hayashi T, Gekka T, Goto-Omoto S, et al. Novel *NR2E3* mutations (R104Q, R334G) associated with a mild form of enhanced S-cone syndrome demonstrate compound heterozygosity. *Ophthalmology* 2005;112:2115–22.

Financial Support: This study was supported by grants from the Ministry of Health, Labour and Welfare of Japan and the Vehicle Racing Commemorative Foundation.

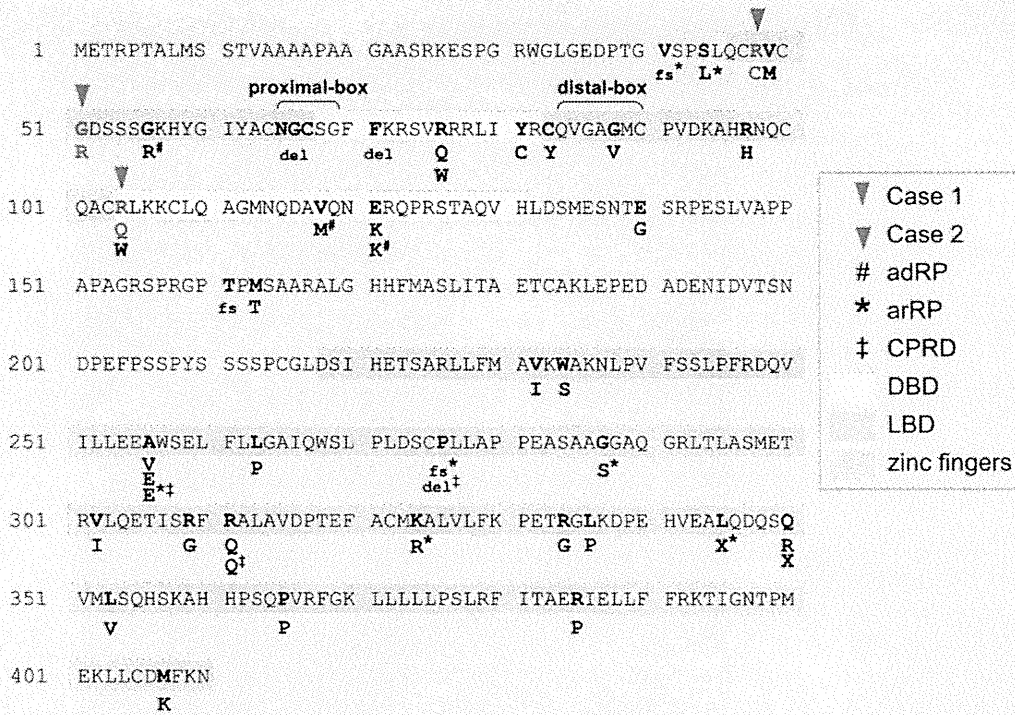
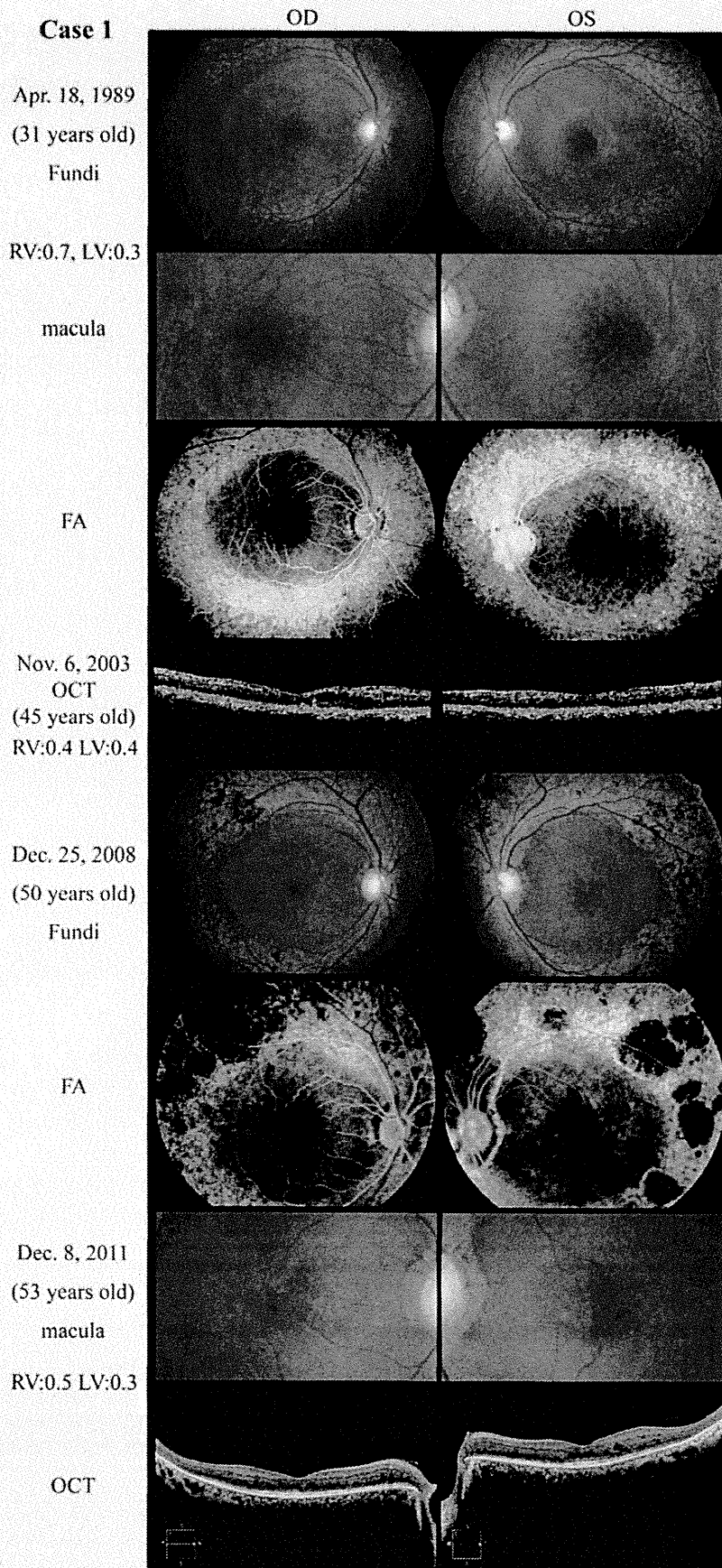


Figure 1. NR2E3 protein structure and mutations in cases presented in this letter and reported in past papers. Bold characters with no marks indicate mutations reported as a cause of enhanced S-cone syndrome (ESCS). Red characters and arrow indicate homozygous missense mutation discovered in Case 1 (p.G51R). Blue characters and arrows indicate compound heterozygous missense mutations discovered in case 2 (p.R48C and p.R104Q). p.G51R and p.R48C are novel mutations as causes of ESCS. adRP = autosomal-dominant retinitis pigmentosa; arRP = autosomal-recessive retinitis pigmentosa; CPRD = clumped pigmentary retinal degeneration; DBD = DNA-binding domain; del = deletion mutation; fs = frame shift of amino acids; LBD = ligand-binding domain.

Letters to the Editor



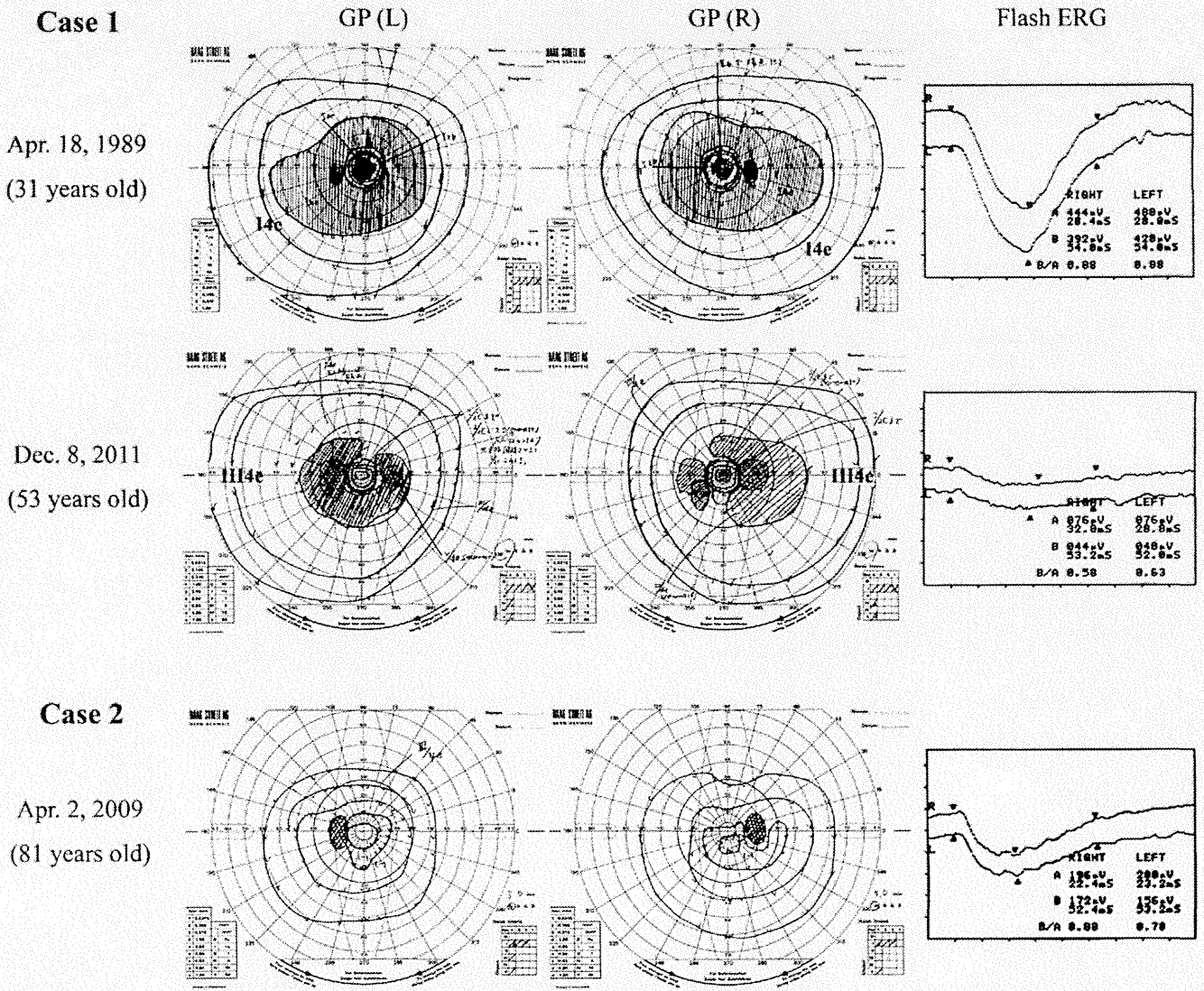


Figure 3. Results of Goldmann perimetry (GP) and flash electroretinography (ERG). In case 1, retinal sensitivity decreased and amplitude of ERG was attenuated during the 2-decade follow-up. In case 2, the visual field and the ERG findings were maintained relatively well in spite of her great age. This figure was made with modification of Figures 2, 3, and 8 in Sato et al.³ with permission.

Figure 2. Results of fundus photography, fluorescein fundus angiography (FA) and optical coherence tomography (OCT) in case 1. At the initial visit (April 1989), cystic changes were observed in the fovea that became ambiguous 2 decades later; vision, however, did not improve. This figure was made with modification of Figures 1 and 6 in Sato et al.³ with permission.

Letters to the Editor

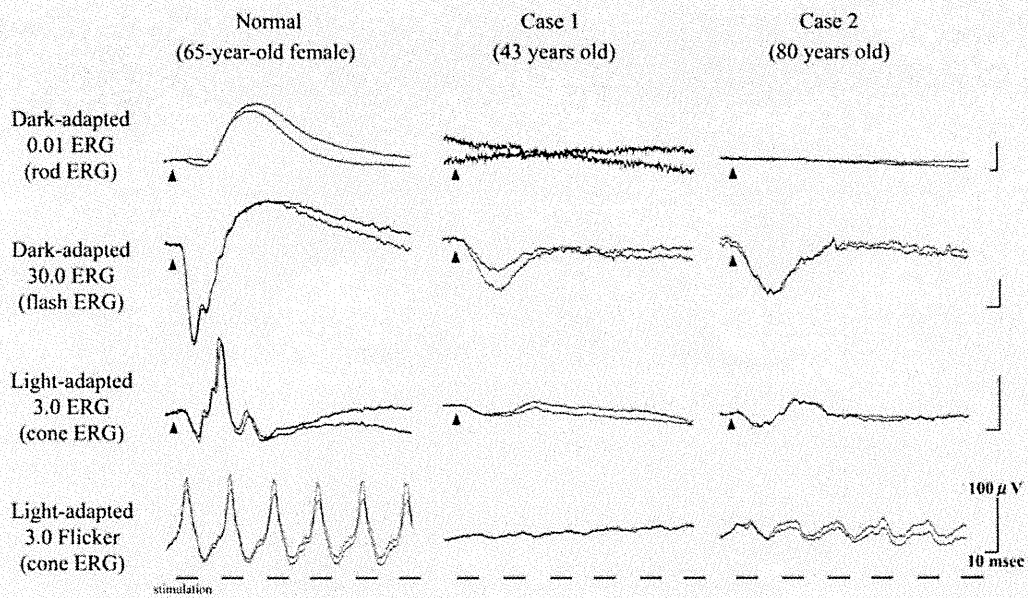


Figure 4. International Society for Clinical Electrophysiology of Vision (ISCEV)-standard electroretinography (ERGs) images. The 2 cases showed nonrecordable rod responses and significantly prolonged flash ERGs. Flicker ERGs derived from the middle- and long-wavelength-sensitive (M- and L-) cone systems were attenuated in these cases. These findings were consistent with enhanced S-cone syndrome. This figure was made with modification of Figure 4 in Sato et al³ with permission.

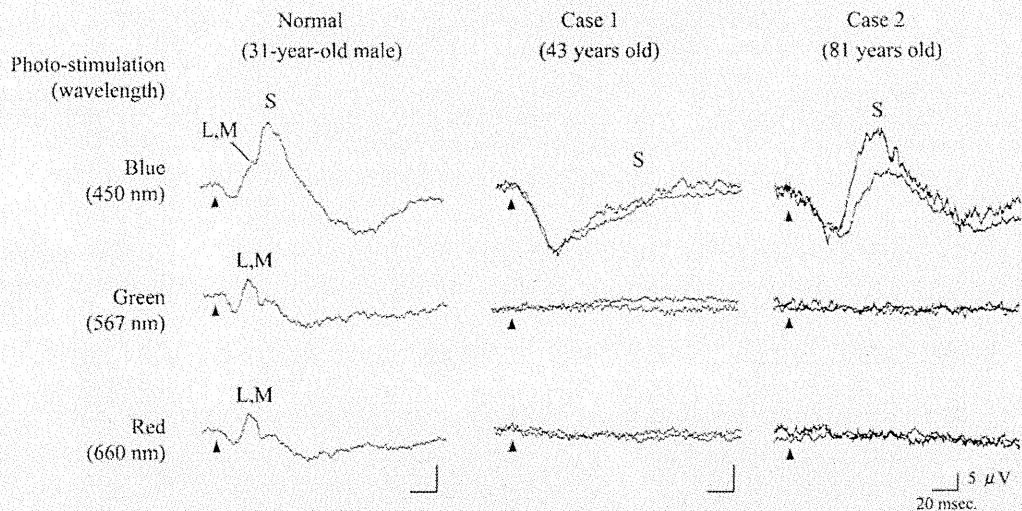


Figure 5. Color electroretinography (ERGs) images. The ERGs were recorded using 3-colored LED-built-in electrode (Kuniyoshi et al. Doc Ophthalmol 2003;106:311-8). The ERGs were elicited by 3 kinds of stimulus, namely, blue, green, and red light under the yellow background light. Luminance of the yellow background light was 670 cd/m² and duration of the stimulus was 2 milliseconds. The ERG waveform elicited by blue stimulus in the normal subject showed double-peaked, namely, rapid b-wave, which was derived from the L- and M-cone systems (L, M) followed by slow b-wave derived from the S-cone system (S). In cases 1 and 2, large b-wave with slow peak time was recorded with blue photostimulation, whereas no response was recorded with green and red photo stimuli. The intensity of the color stimulus was decided to elicit the rapid b-wave (L, M) with almost the same amplitude as in the normal subject. This Figure was made with modification of Figure 5 in Sato et al³ with permission.

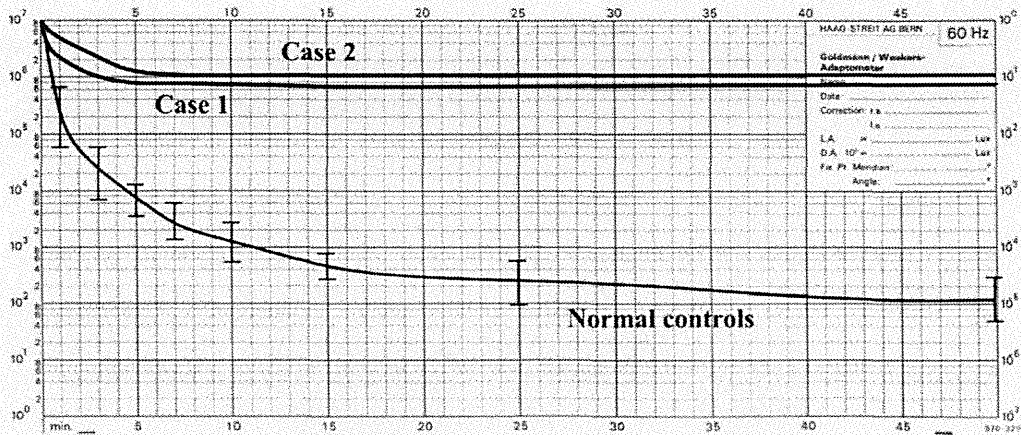


Figure 6. Results of Goldmann-Weekers dark adaptometry. Lower line indicates averaged value and its standard deviation resulted from normal controls.

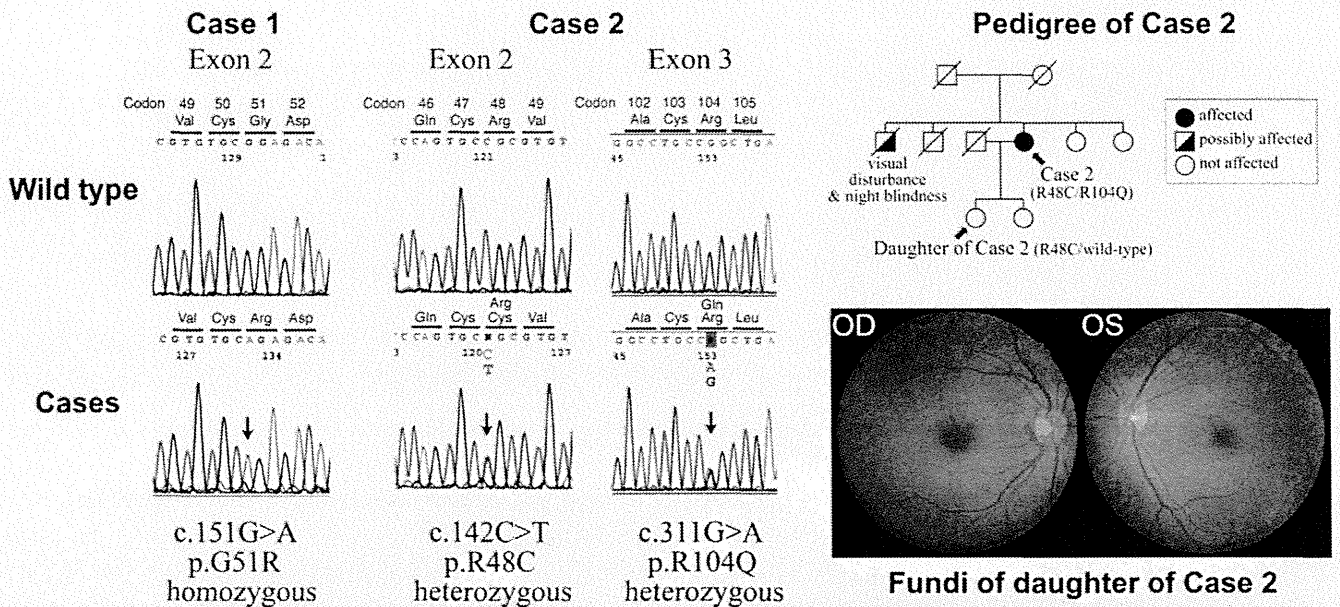


Figure 7. Results of DNA sequencing of the *NR2E3* gene in cases 1 and 2 (left), the pedigree of case 2, and fundus photographs of the daughter of case 2 (right). Mutation analysis identified a novel homozygous missense mutation of p.G51R, which resides in the DNA-binding domain (DBD) in *NR2E3* protein in case 1. In case 2, heterozygous missense mutation of p.R48C and p.R104Q were identified, and the former is a novel mutation. A daughter of case 2 revealed heterozygous missense mutation of p.R48C and normal fundus appearance. In mutation screening of the *NR2E3* gene, all coding exons including exon/intron boundaries were amplified using polymerase-chain reaction (PCR) with primer pairs followed by sequencing. The primers and protocols used for PCR, and the procedures of PCR amplification and purification were the same as reported previously.⁵

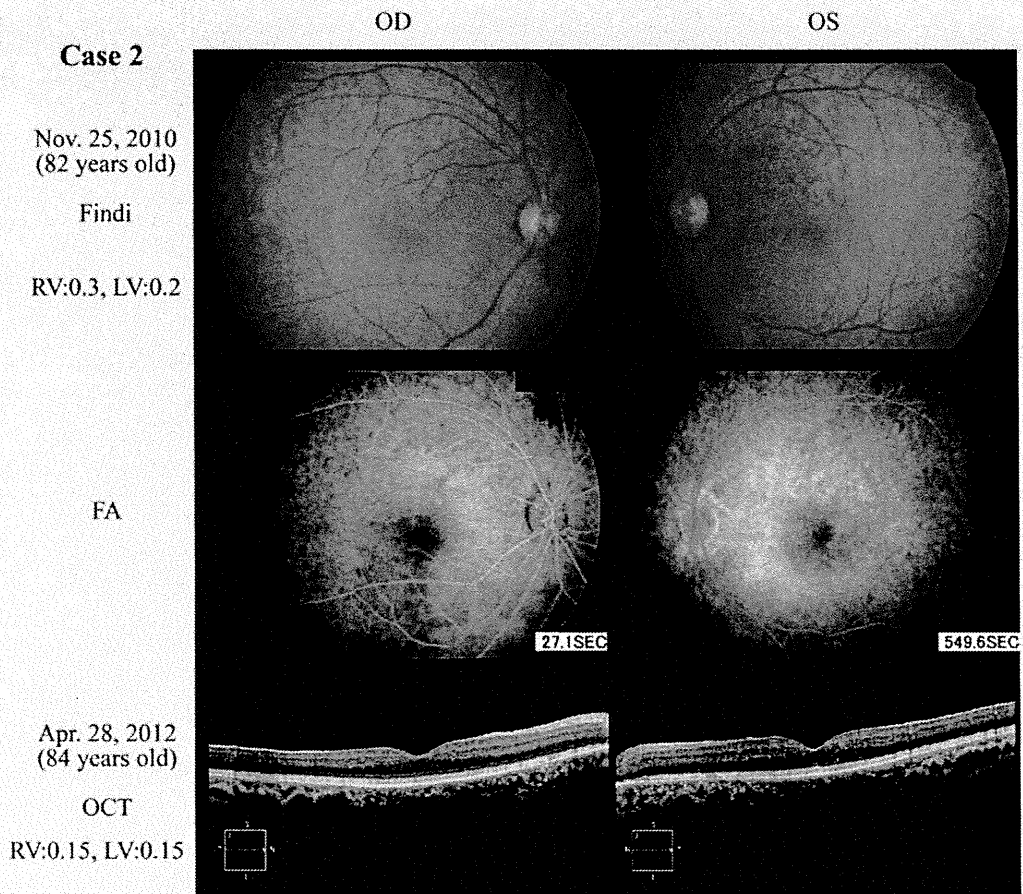


Figure 8. Results of fundus photography, fundus angiography (FA), and optical coherence tomography (OCT) in case 2. These photographs were taken after cataract surgery. The retinal degeneration was relatively mild with no pigmentation in both eyes. This Figure was made with modification of Figure 7 in Sato et al³ with permission.